 adova - 2020

SAND2020-1887C

Theoretical and experimental study of breakdown delay time in pulse discharge

Irina Schweigert[1], Matthew Hopkins[2], Edward Barnat[2] and Michael Keidar[1]

[1] The George Washington University, Washington DC, USA
[2] Sandia National Laboratories, Albuquerque, NM, USA

PIC MCC simulation results on the breakdown in the pulse discharge in helium at pressure of 100 Torr and voltage of U=3.25 kV are presented. The delay of the breakdown development is studied with different initial densities of plasma and excited helium atoms, which corresponds to various discharge operation frequencies. It is shown that for high concentration of excited atoms the photoemission determines the breakdown delay time. In opposite case of low excited atoms density, the ion-electron emission plays a key role in the breakdown development. The photoemission from the cathode is set with a flux of the photons with Doppler shift over the frequency. These photons are generated in reactions between exited atoms and fast atoms. A wide distribution of breakdown delay time was observed in different runs and analyzed.

***Index Terms*—Gas discharge, breakdown delay time, simulations, electron emission**

I. Introduction

In pulse discharges with the operation frequency of 1 – 100 Hz the breakdown delay time after applying the working voltage has stochastic nature. For example, in helium pulse discharge at gas pressure of 100 Torr the breakdown delay time varies from 0.1 to 10 microseconds. The mechanism responsible for the discharge current evolution is still not clear. In this study in PIC MCC simulation we study the evolution of discharge current for different initial plasma conditions. The discharge operates at voltage U=3.25 kV and gas pressure P = 100 Torr.

II. Theoretical Model

In our simulations, the system of equations describes the discharge breakdown for a wide range of gas pressures and voltages. It includes three Boltzmann equations for distribution functions of electrons, ions and fast atoms and Poisson equation for the electrical potential distribution. The collision set for electrons, ions and fast atoms include elastic scattering, excitation and ionization of He background atoms. Additionally for fast atoms, the collisional excitation transfer reactions, He* + He(fast) = He + He*(fast)= He + He(fast)+hv(DS) is included. The cross section of this reaction is large [1]

$$\sigma_r = 4.6\times10^{-14}/\varepsilon_a^{1/2}\ \mathrm{cm}^2,$$

and photons with Doppler shift over the frequency efficiently produced in these types of reactions. In the discharges in helium the coefficient of photoemission from the electrode can be as large as 0.3 [2,3]. In plasma devices the surfaces treated by energetic heavy particles, is contaminated and photoemission coefficient can be an order of magnitude higher than one measured at vacuum conditions [4,5].

In our PIC MCC simulation, the inter electrode gap is 1.1 cm. The voltage front rise is 20 ns or 2 ns. The initial density of helium atoms He* excited by the energetic electron is $n^*=10^{10}$ cm^{-3} or 7×10^{11}cm^{-3}. The maximum density of plasma is $n=2\times10^{7}$cm^{-3} or 2×10^{8}cm^{-3}. The initial distributions of electron and ions densities are calculated for the conditions of plasma decay in afterglow at U=0.

The electron emission from the electrode surface is considered to be due to ion-electron emission ($\gamma_{i\text{-}e}$), fast atom-electron emission ($\gamma_{a\text{-}e}$), secondary electron emission ($\gamma_{e\text{-}e}$), and photoemission. These coefficients of electron emission are functions of the energy of bombarding particles. The system of equations was solved with the 1D3V PIC MCC method with code developed by I.V. Schweigert [4].

III. Simulation Results

In the beginning the initial plasma density is small and the potential distribution over the inter electrode gap is almost linear. The voltage increases during 20 ns and electrons are accelerated to the anode direction. At P=100 Torr, the mean free pass of electrons for inelastic collisions is about 0.01 cm and electrons gain energy about 30 eV. At this stage 1, the ionization is practically uniform over the gap and the discharge current increases. In Figure 1, the discharge current evolution is shown for three different runs for a 20 ns voltage front rise, $n^*=10^{10}$ cm^{-3} and $n=2\times10^{7}$cm^{-3}. All runs demonstrate the same breakdown scenario, but the different breakdown delay time τ_d. Note that for all runs the initial

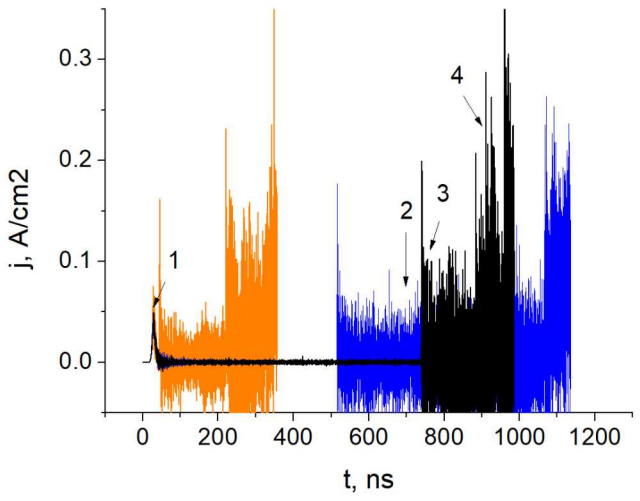

Fig. 1. Discharge current with time for different runs. 1, 2, 3 and 4 show different stages of discharge current development.

conditions were the exactly the same. The further analysis will be done for the run shown in black in Figure 1.
As seen in Figure 1, after stage 1, the discharge current drops (stage 2) and remains small till the ion-electron emission starts. At this point (stage 3), the discharge current noise essentially increases. At stage 4, the discharge current rises by factor of 2-3 and it is related to the enhanced electron emission from the cathode.

In Figure 2, the electrical potential distribution is shown for stages 1-4 shown in Figure 1. The cathode is at z=1.1 cm. Almost linear potential distribution (1) is followed by the formation of the cathode sheath (cathode is at z=1.1 cm). The potential profile with a step corresponds to the stage 3, when the plasma profile is bimodal. The potential profile at the moment of the breakdown is denoted by the number 4. The cathode sheath thickness is 0.1 cm and the mean energy of electrons considerably increases within the cathode sheath.

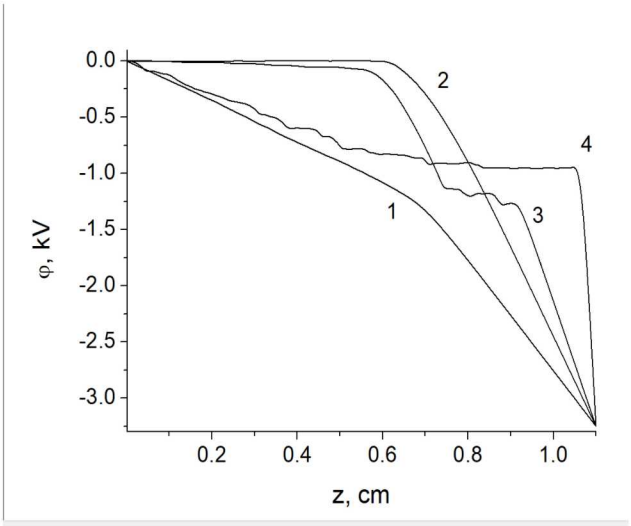

Fig. 2. Electrical potential distribution for the discharge current development for stages 1-4 shown in Fig.1.

The averaged electron energy distribution for the stages 1-4 is shown in Figure 3. The electrons have the mean energy of 10 eV for the case of the linear potential distribution (stage 1). The maximum electron energy of 200 eV is in the cathode sheath at stage 4.

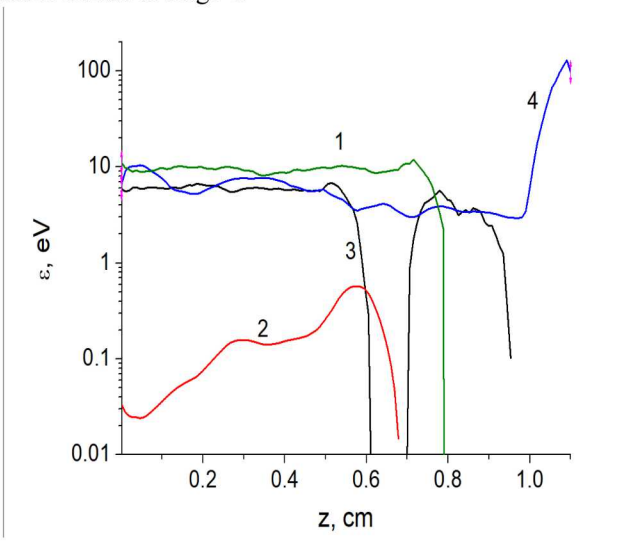

Fig. 3.Mean electron energy distribution for stages 1-4 shown in Fig.1.

The electron and ion density profiles are shown in Figure. 4 at different times of the breakdown development. During first 30 ns the plasma density increases from $2x10^7 cm^{-3}$ to $5x10^{10} cm^{-3}$. Then during the stage 2, the maximum of plasma density remains the same. The cathode sheath increases because the electrons is shifting to the anode direction and ions to the cathode. It is know, that the value of the breakdown threshold in helium is E/P=13 V/cmTorr. In our discharge, there is E/P=30 V/cmTorr in the liner stage 1 and ~15 V/cmTorr at the stage 2. The averaged ion velocity is ~ $1.4x10^5$cm/s, that means that an ion can cross the cathode sheath for 6-7 microseconds to provide ion-electron emission. For efficient photoemission, it is necessary to produce a large concentration of fast atoms for the collisional excitation transfer reactions.

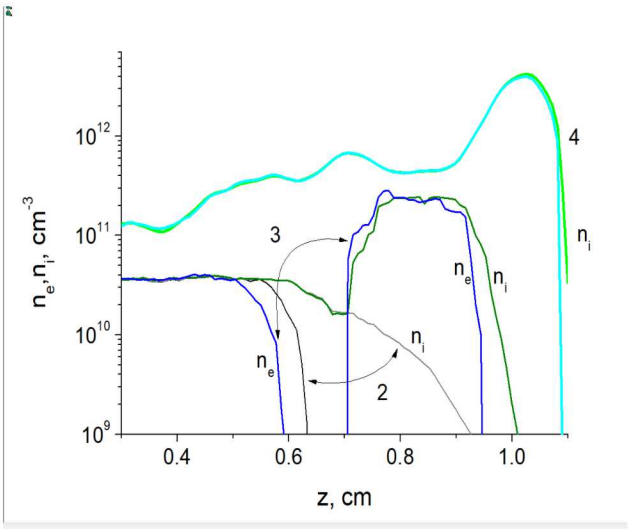

Fig. 4. Concentration of electrons and ions distribution for stages 2, 3 and 4 shown in Fig.1.

In Figure 5, the distributions of densities of excited helium atoms and fast atoms are shown. It is seen that at the stage 4 both densities increases essentially and the contribution of photons in the electron emission becomes dominant.

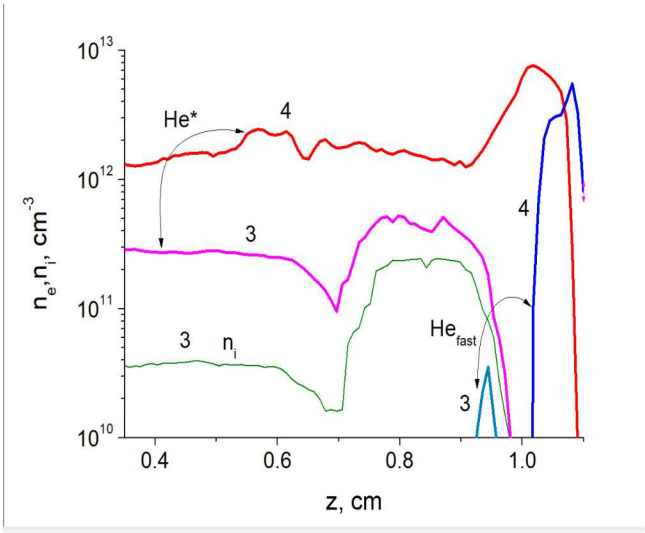

Fig. 5. Distributions of densities of excited atoms He* and fast atoms for stages 3 and 4 shown in Fig.1.

The electron emission currents from the cathode due to ion-electron and photoemission are shown in Figure 6. First, the ion-electron emission dominates and then the photoemission switches on. For these initial conditions the averaged breakdown delay time is 1300 ns. This value was calculated from 20 runs with exactly the same initial conditions.

For different initial conditions, for example, for higher initial density of the excited atoms, $7x10^{11}cm^{-3}$, the breakdown delay time τ_d is much shorter, and governed mainly by photoemission. In PIC MCC simulations, we also checked the effect of time of voltage rise. For the 2 ns voltage front rise, with the initial $n^*=7x10^{11}cm^{-3}$, τ_d= 150 ns.

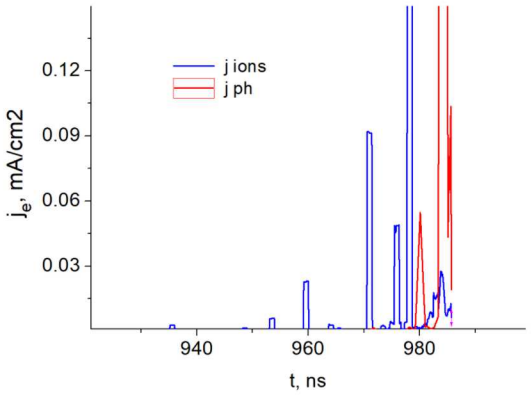

Fig. 5. Emission current with time due to ion-electron emission and photoemission with DS photons for the run with numbers 1-4 shown in Fig.1.

An increase of the initial plasma density from $2x10^7cm^{-3}$ to $2x10^8cm^{-3}$ also reduces τ_d .

IV. Conclusion

The aim of this study is to understand the statistical spread of times of breakdown delay in different discharge runs observed previously and in our experiments. In PIC MCC simulations, the discharge breakdown development at U=3.25 kV and P=100 Torr in helium was studied for various initial plasma conditions. For all cases, the same breakdown scenario was found. In the beginning, in the first stage, the density of plasma is small and the potential distribution is linear. The electrons gain energy in the uniform electrical field, the ionization starts and discharge current increases. With further increase of the plasma density, the cathode sheath forms and the discharge current drops (stage 2). The ions from 'the initial afterglow distribution' reach the cathode surface and provides the electron emission current. This ion flux is small since the ion density near the cathode is set by the plasma decay in afterglow. At this stage 3, the plasma has a bimodal distribution. There is a group of thermalized electrons and ions in quasineutral part (close to anode) in which the electrons are slowly drifting to the anode. Another group (close to cathode) of electrons and ions is produced by ionization with the electrons emitted from the cathode. This part of plasma has much higher density and electrons are trapped by ion charge. The potential has a stepwise profile. At the stage 4 (discharge breakdown), the production of photons from collisional excitation transfer reactions rise and the ion flux increases that leads to the breakdown.

Acknowledgment

We wish to thank National Science Foundation Industry/University Cooperative Research Center for financial support. Sandia National Laboratories is a multimission laboratory managed and operated by National Technology & Engineering Solutions of Sandia, LLC, a wholly owned subsidiary of Honeywell International Inc., for the U.S. Department of Energy's National Nuclear Security Administration under contract DE-NA0003525. This paper describes objective technical results and analysis. Any subjective views or opinions that might be expressed in the paper do not necessarily represent the views of the U.S. Department of Energy or the United States Government.

References

[1] I. Sobel'man, L. A. Vainstein, and E. A. Yukov, Excitation of Atoms and Broadening of Spectral Lines (Nauka, Moscow, 1979; Springer-Verlag, Berlin, 1981)

[2] P. A. Bokhan and Dm. E. Zakrevsky, Tech. Phys., 52, 104 (2007).

[3] P. A. Bokhan and Dm. E. Zakrevsky, Phys. Rev. E, 88, 013105 (2013).

[4] A. Phelps and Z. Petrovic, Plasma Sources Sci. Technol., 8, R21 (1999).

[5] L. N. Dobretsov and M. V. Gomoyunova, Emission Electronics (Israel Program for Scientific Translations, Jerusalem, 1971).

[6] I. V. Schweigert, A. L. Alexandrov, Dm. E. Zakrevsky, P. A. Bokhan, Mechanism of Formation of Subnanosecond Current Front in High-Voltage Pulse Open Discharge, Phys. Rev. E 90, 051101(R) (2014)

E-mail of the author(s): ivschweigert@email.gwu.edu